# Analysis of the effects of fibre and moisture content on the impedance response of cement-based sensors

Jiacheng Zhang[1]*, Andrew Heath[1], Richard J. Ball[1], Kevin Paine[1]
[1]*Department of Architecture & Civil Engineering, University of Bath, Claverton Down, Bath BA2 7AY, United Kingdom*
* Email(s): jz2031@bath.ac.uk

## ABSTRACT

The influence of fibre and moisture content on the electrical properties of cement-based sensors (cement mortars incorporating milled carbon fibres) with a percolation zone from 0.55 to 1.29 vol. % has been studied. Under drying conditions, cement-based sensors produced more stable electrical behaviour than plain mortars. Two-point AC impedance measurement was employed to study the dielectric polarizability and bulk conductivity of cement-based sensors, which were both found to be enhanced upon fibre inclusion, and the enhancement of conductivity became more pronounced towards higher frequencies. We propose the characteristic bulk conductivity can be obtained at 100 kHz for cement-based sensors.

## 1. INTRODUCTION

Intrinsic self-sensing concrete (cement-based sensor) can provide accurate, real-time assessment allowing identification and thereafter remediation of defects, increasing the life of structures. Electrically conductive fibres (e.g. Carbon fibres, Steel fibres, Carbon nanotubes) are dispersed in cement matrix to enhance the overall electrical conductivity and flexural strength and to form an "active" sensing network. Through this network, the composite becomes multifunctional in that it not only has excellent structural performance but also has the ability to monitor strain/stress, crack, temperature, and moisture content changes. Cement-based sensors have been extensively studied with respect to fracture strength and self-sensing functionality under laboratory conditions [1-5]. Under field conditions, the ambient temperature and humidity can have a significant influence on the electrical behaviour, therefore environmental effects need to be investigated to allow the development of self-sensing concrete.

A cement-based sensor is essentially a conductive phase (conductive fibres) dispersed in a semi-conductive phase (cement matrix). Such composites, if heterogeneous, are suitable for investigation by impedance spectroscopy. Both conductivity $\sigma(\omega)$ and relative permittivity $\varepsilon_r(\omega)$ are associated with electronic and electrolytic mechanisms, thus reflecting component properties. The electrical behaviour of cement-based sensors can be studied more effectively under field conditions when the conductivity is enhanced.

## 2. MATERIALS AND METHODS

### *2.1 Materials*

Mortar matrices were prepared with CEM II/A-L 32.5R, deionized water, and standard sand of maximum particle size 2 mm (BS EN 196-1). Pitch-based milled carbon fibres of diameter 7.5 μm, length 100 μm, density 1.8 g/cm$^3$, tensile strength 3150 MPa and modulus 200 GPa (Easy Composites Ltd, Stoke-on-Trent, UK) were used as conductive fillers. Stainless steel (Type 316, Avery Knight & Bowlers Engineering Ltd, Bath, UK) electrodes were used for their ability to resist the alkaline cement environment and ensure changes in the electrodes did not affect results.

### *2.2 Manufacturing*

Cement-based sensors were made with fibres of bulk volume fractions from 0.00 vol. % to 1.93 vol. % (cubic samples, 40×40×40 mm); with 0.33 vol. % used for prismatic sensors (40×40×160 mm) to aid studies of moisture content [6]. Standard mix proportioning of 450 g (cement), 225 g (water), 1350 g (sand) was employed. Ultrasonic bathing was used to promote fibre dispersion reducing the influence of admixtures [5]: a sealed glass bottle containing all fibres and a small portion of water was initially bathed in an ultrasonicator for 30 minutes. BS EN 196-1 was then followed with the exception of extended time when mixing the fibre-water solution and wet cement mix. Electrodes were inserted into the specimens after casting into moulds (Figures 1 and 2). All samples were demolded after 24 hours and cured in a water tank. Pristine and cured states of each specimen varied and will be discussed in more detail in the next section.

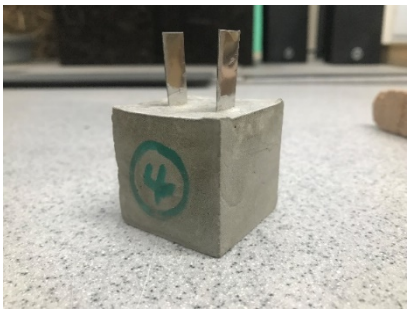

***Figure 1.*** *Cubic samples*

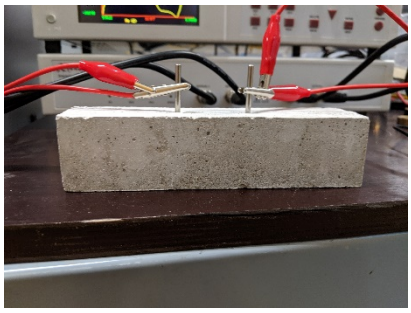

***Figure 2**. Prism samples under two-point impedance measurement*

### *2.2 Manufacturing*

Electrical impedance measurements were taken using a Newtons4th PSM 3750 impedance spectrometer. A voltage amplitude of 2 V over the frequencies 1 Hz – 10 MHz sweeping logarithmically with 10 points per decade was used. Cubic samples removed from the water tank were tested weekly from 7 to 49 days after casting and stored in an environmental chamber (50 ± 10% RH; 25 ± 5 ºC) between measurements. Prism samples were removed at 28 days after casting and dried with an electronic fan at 20 ± 3 ºC until the 9th week following initial saturation. The impedance and moisture content were measured weekly. As the average volume resistivity was of interest and the uniformity of current distribution is strongly related to the moisture content distribution within the matrix, each sample was placed in a zip-lock bag for 6 hours to facilitate equalization of the moisture distribution prior to each impedance measurement. The moisture content was determined by equation 1:

$$Moisture\ \% = \frac{W_t - W_{dry}}{W_{dry}} \times 100\% \qquad \text{Equation 1}$$

where $W_t$ is the weight at a certain time, $W_{dry}$ is the dry weight and was obtained at 7 days of 50 ºC oven time.

A two-point AC impedance setup was used as four-point AC measurements were found to be problematic due to current leakage [7, 8]. Conductivity $\sigma\ (\omega)$ and relative permittivity $\varepsilon_r(\omega)$ were calculated using equations 2 and 3 [8]:

$$\sigma\ (\omega) = \frac{Z'(\omega)}{[Z'(\omega)]^2 + [Z''(\omega)]^2} \cdot \frac{kd}{A} \qquad \text{Equation 2}$$

$$\varepsilon_r(\omega) = \frac{Z''(\omega)}{\varepsilon_0 \omega \{[Z'(\omega)]^2 + [Z''(\omega)]^2\}} \cdot \frac{kd}{A} \qquad \text{Equation 3}$$

where Z'(ω) is the real (resistance) component and Z"(ω) is the imaginary (reactance) component of impedance, $\varepsilon_0$ is the permittivity of vacuum and equals to $8.854 \times 10^{-12}$ F/m, A is sample cross-section area perpendicular to the electric field, d is the distance between the sensing electrodes, and k is a conversion factor associated with electrode geometry. Although the embedded electrodes give a closer contact to the matrix and acquire more volume information, such setups are influenced by field fringing [9]. The factor k was determined using a sample from the same batch by a four-point technique [10], with an electrode area A. Values of 3.2 and 1.6 were obtained for cubic and prism samples, respectively.

## 3. RESULTS AND DISCUSSION

Representative impedance responses (Nyquist plot) of the plain mortar and cement-based sensor are presented in Figure 3. The impedance response of hardened cement has been extensively studied, which is typically a low-frequency electrode "spur" followed by a high-frequency bulk arc where the bulk resistance $R_{b0}$ can be obtained at their intersection [11, 12]. Upon fibre inclusion, a small arc emerges between the bulk arc and electrode "spur" where the bulk resistance $R_{bcf}$ is obtained at the intersection of bulk and small arcs [13].

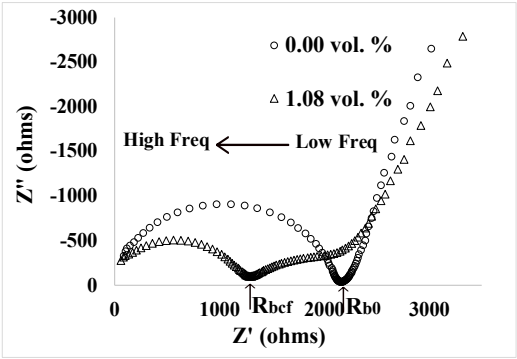


***Figure 3.** Typical Nyquist plot of plain mortar and cement-based sensor containing milled carbon fibres*

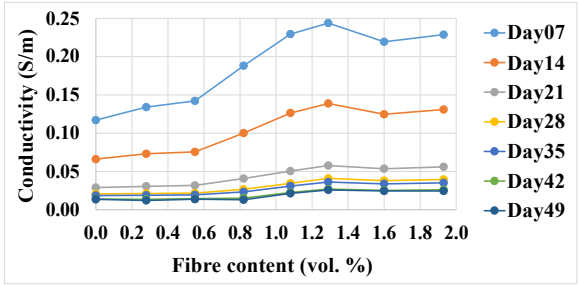


***Figure 4.** Variations of conductivity of cement-based sensors with different fibre content over time.*

The development of electrical conductivity is plotted in Figure 4. Regardless of the curing age, the conductivity undergoes a significant increase between a fibre content of 0.55 vol. % and 1.29 vol. %; but has marginal changes outside of this zone. This region, known as the percolation zone, has been observed to take place at lower volume fractions from 0.50 to 1.00 vol. % in [6] for longer fibres. In this case, fibres are more likely to be in direct contact with each other and form continuous conductive paths throughout the cement matrix thus enhancing the bulk conductivity. Above this region conductivity enhancement is not observed due to difficulties associated with dispersing at higher fibre content. Fibres high in aspect ratios promote agglomeration in the porous cement medium, therefore a low fibre content or additional dispersion methods at higher fibre contents to aid uniform

dispersion is of benefit [6, 16].

A heterogeneous material has various electrochemical mechanisms operating simultaneously over a specific range of frequencies where each is characterized by a relaxation frequency. Such dispersive behaviour is observed in the frequency domain where dielectric permittivity falls and conductivity rises as shown in Figures 5 and 6. Figure 5 shows that relative permittivity decreases from 1 Hz before reaching a plateau at frequencies above 100 kHz, irrespective of fibre content, indicating that the bulk permittivity can be determined over this value. Relative permittivity increases with fibre content over the frequency range 50 Hz – 100 kHz, which is associated with enhanced polarizability. A greater number of fibres increase fibre-matrix, fibre-fibre interfacial area, providing more surfaces for charge polarization thereby enhancing the dielectric polarizability and relative permittivity [8, 13, 14]. In Figure 6, the conductivity enhancement becomes discernible at frequencies above 1 kHz with increasing fibre content. Compared to the reference sample (0.00 vol. %) which has a plateau region between 1 kHz and 100 kHz, samples containing fibres appear to be enhanced in conductivity incrementally over this frequency range. A continuous conductive network can form as the fibre content increases, providing electronic conduction enhancing conductivity. In addition, the increased area of polarization will result in the enhancement of bulk polarizability, which can also lead to more marked enhancement of conductivity at higher frequencies [8].

Under site conditions, variations of ambient humidity will influence the moisture content of concrete and its self-sensing behaviour. To understand this better a drying study was carried out on cement-based sensors containing 0.33 vol. % milled carbon fibres. Figure 7 shows that the sensors exhibit an increase in electrical resistivity (1-0.33 vol. % and 2-0.33 vol. % are from the same batch) as moisture content decreases. Compared to the reference sample, the cement-based sensors have lower moisture content decreasing rate as well as lower increment of resistivity. Cement-based sensors lost 3.8 % of their moisture compared to 4.5% for the reference sample while the resistivity increased by 400 Ω compared to 2000 Ω for the reference sample. Since the fibre content is below that required for percolation, it can be assumed that there is no direct fibre-fibre contact in this case. Therefore, the electrolytic conduction still dominates, and the moisture content should have a major impact on resistivity. It was hypothesized by [15] that when the fibre-cement interface and fibres are sufficiently close to each other electronic conduction or transmission may operate. In a cement matrix, fibres may form bridges across pores allowing electronic conduction and a tunnelling effect by operating between holes and electrons on the fibre surface. These two electronic phenomena are independent of the mobility of free ions which the polarizability and conductivity of plain mortars have a positive relationship with.

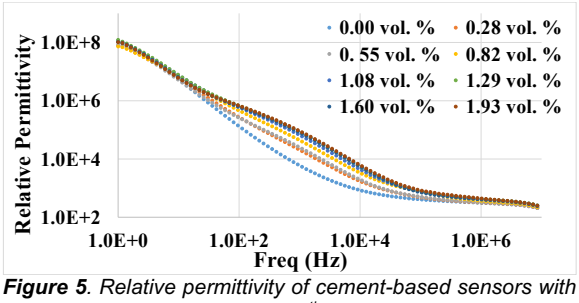


***Figure 5**. Relative permittivity of cement-based sensors with different fibre contents on the 35th day*

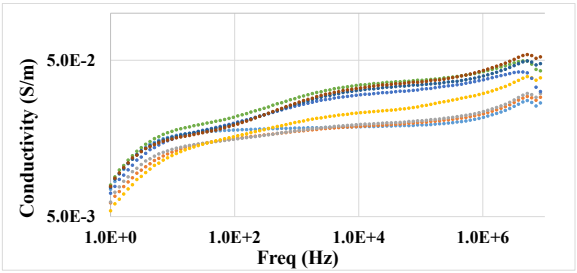


**Figure 6**. Conductivity of cement-based sensors with different fibre contents on the 35th day

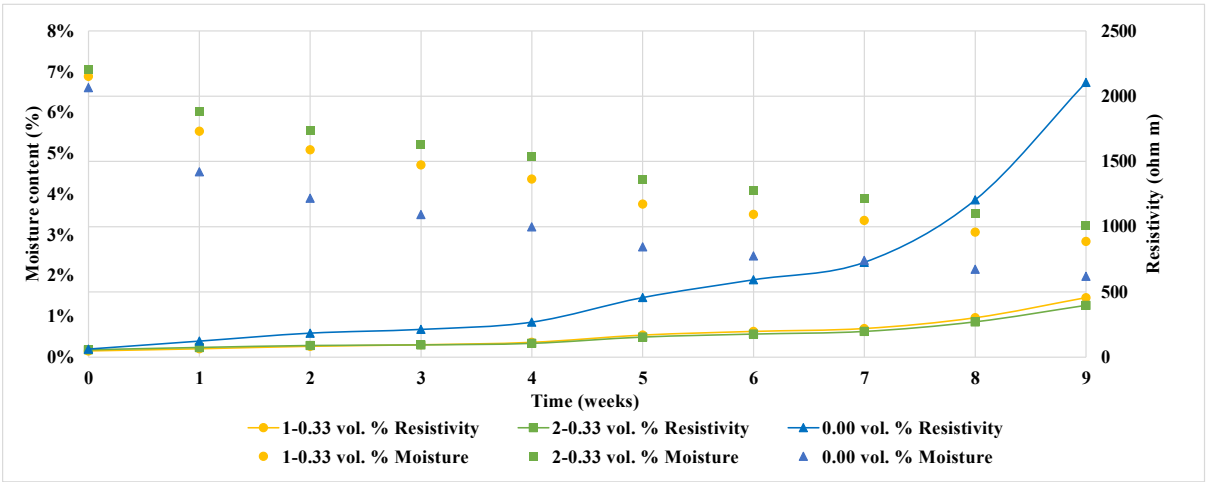


***Figure 7**. Variations of moisture content and electrical resistivity of plain mortar and cement-based sensors for a 9-week fan drying period*

## 4. CONCLUSIONS

The influence of fibre and moisture content on a sensor with a percolation zone of 0.55 vol. % to 1.29 vol. % was determined. This region was a function of fibre properties and the cement matrix composition, indicating that the percolation threshold should be determined prior to testing. Impedance spectroscopy indicated that increased active sites for dielectric polarization in the presence of fibres contributed a more pronounced conductivity enhancement in the high-frequency domain. Therefore, it is suggested that the conductivity of cement-based sensors can be obtained at 100 kHz in contrary to plain mortar's low-frequency feature. Cement-based sensors exhibited electrical properties with a lower moisture dependence when compared to plain mortar. This could allow more accurate assessment of concrete conditions when utilised in the field, enabling its potential for further environmental tests.

## 5. ACKNOWLEDGEMENTS

The Engineering and Physical Sciences Research Council (EPSRC; EP/PO2081X/1) and industrial collaborators/partners are thanked for funding the Resilient Materials for Life (RM4L) project.

## 6. REFERENCES

1. Banthia N, Djeridane S, Pigeon M (1992) Electrical resistivity of carbon and steel micro-fiber reinforced cements. Cem. Concr. Res. 22:804-814.
2. Chung D (1995) Strain sensors based on the electrical resistance change accompanying the reversible pull-out of conducting short fibers in a less conducting matrix. Smart Mater. Struct. 4:59-61.
3. Han B, Guan X, Ou J (2007) Electrode design, measuring method and data acquisition system of carbon fiber cement paste piezoresistive sensors. Sens. Actuators, A 135:360-369.
4. Han B, Ding S, Yu X (2015) Intrinsic self-sensing concrete and structures: A review. Measurement 59:110-128.
5. Azhari F, Banthia N (2012) Cement-based sensors with carbon fibers and carbon nanotubes for piezoresistive sensing. Cem. Concr. Compos. 34:866-873.
6. Chung D (2005) Dispersion of Short Fibers in Cement. J. Mater. Civ. Eng. 17:379-383.
7. Anderson E, Bühlmann P (2016) Electrochemical Impedance Spectroscopy of Ion-Selective Membranes: Artifacts in Two-, Three-, and Four-Electrode Measurements. Anal. Chem. 88:9738-9745.
8. McCarter W, Starrs G, Chrisp T, Banfill P (2009) Complex Impedance and Dielectric Dispersion in Carbon Fiber Reinforced Cement Matrices. J. Am. Ceram. Soc. 92:1617-1620.
9. Ball R, Allen G, Starrs G, McCarter W (2011) Impedance spectroscopy measurements to study physio-chemical processes in lime-based composites. Appl. Phys. A 105:739-751.
10. McCarter W, Taha H, Suryanto B, Starrs G (2015) Two-point concrete resistivity measurements: interfacial phenomena at the electrode–concrete contact zone. Meas. Sci. Technol. 26:085007.
11. McCarter W, Brousseau R (1990) The A.C. response of hardened cement paste. Cem. Concr. Res. 20:891-900.
12. Christensen B, Coverdale T, Olson R, Ford S, Garboczi E, Jennings H, Mason T (1994) Impedance Spectroscopy of Hydrating Cement-Based Materials: Measurement, Interpretation, and Application. J. Am. Ceram. Soc. 77:2789-2804.
13. Torrents JM, Mason TO, Garboczi EJ (2000) Impedance spectra of fiber-reinforced cement-based composites: a modeling approach. Cem. Concr. Res. 30:585–592.
14. Díaz B, Guitián B, Nóvoa X, Pérez C (2020) Analysis of the microstructure of carbon fibre reinforced cement pastes by impedance spectroscopy. Constr. Build. Mater. 243:118207.
15. Sun M, Li Z, Mao Q, Shen D (1998) Study on the Hole Conduction Phenomenon in Carbon Fiber-Reinforced Concrete. Cem. Concr. Res. 28:549-554.
16. Chen P, Chung D (1995) Improving the electrical conductivity of composites comprised of short conducting fibers in a nonconducting matrix: The addition of a nonconducting particulate filler. J Electron Mater 24:47-51.